AGU PUBLICATIONS

Geophysical Research Letters

RESEARCH LETTER
10.1002/2015GL065293

Special Section:
First Results from the MAVEN Mission to Mars

The spatial distribution of planetary ion fluxes near Mars observed by MAVEN

D. A. Brain[1], J. P. McFadden[2], J. S. Halekas[3], J. E. P. Connerney[4], S. W. Bougher[5], S. Curry[2], C. F. Dong[5], Y. Dong[1], F. Eparvier[1], X. Fang[1], K. Fortier[1], T. Hara[2], Y. Harada[2], B. M. Jakosky[1], R. J. Lillis[2], R. Livi[2], J. G. Luhmann[2], Y. Ma[6], R. Modolo[7], and K. Seki[8]

[1]Laboratory for Atmospheric and Space Physics, University of Colorado Boulder, Boulder, Colorado, USA, [2]Space Sciences Laboratory, University of California, Berkeley, California, USA, [3]Department of Physics and Astronomy, University of Iowa, Iowa City, Iowa, USA, [4]NASA Goddard Space Flight Center, Greenbelt, Maryland, USA, [5]Department of Atmospheric, Oceanic, and Space Sciences, University of Michigan, Ann Arbor, Michigan, USA, [6]Institute of Geophysics and Planetary Physics, University of California, Los Angeles, California, USA, [7]UVSQ/LATMOS-IPSL/CNRS-INSU, Guyancourt, France, [8]Solar-Terrestrial Environment Laboratory, Nagoya University, Nagoya, Japan

Abstract We present the results of an initial effort to statistically map the fluxes of planetary ions on a closed surface around Mars. Choosing a spherical shell ~1000 km above the planet, we map both outgoing and incoming ion fluxes (with energies >25 eV) over a 4 month period. The results show net escape of planetary ions behind Mars and strong fluxes of escaping ions from the northern hemisphere with respect to the solar wind convection electric field. Planetary ions also travel toward the planet, and return fluxes are particularly strong in the southern electric field hemisphere. We obtain a lower bound estimate for planetary ion escape of $\sim 3 \times 10^{24}\ s^{-1}$, accounting for the ~10% of ions that return toward the planet and assuming that the ~70% of the surface covered so far is representative of the regions not yet visited by Mars Atmosphere and Volatile EvolutioN (MAVEN).

Key Points:
- MAVEN ion measurements are mapped to a spherical surface around Mars
- Planetary ion fluxes are organized in four spatial regions on the shell
- Heavy ion escape rates exceed $2 \times 10^{24}\ s^{-1}$ for energies >25 eV

Correspondence to:
D. A. Brain,
david.brain@lasp.colorado.edu

Citation:
Brain, D. A., et al. (2015), The spatial distribution of planetary ion fluxes near Mars observed by MAVEN, *Geophys. Res. Lett.*, *42*, doi:10.1002/2015GL065293.

Received 8 JUL 2015
Accepted 18 SEP 2015

1. Introduction

The escape of atmospheric particles to space may have been especially effective at Mars, relative to Earth or Venus, due to a combination of its small size and lack of global magnetic field. The small size leads to a low escape energy for atmospheric particles, and the lack of global magnetic field allows the incident solar wind to approach much closer to the planet than at Earth, so that the solar wind interacts directly with the Martian upper atmosphere. Considering that planetary ions may be more effectively removed from the atmosphere in this interaction, a major goal over the past few decades has been to accurately evaluate the loss of ions from Mars under a variety of solar and solar wind conditions. One reason for doing so is to determine whether an early greenhouse atmosphere could have been removed over billions of years, causing the Martian climate to transition from a state that allowed liquid water to play a prominent role in shaping the surface to today's inhospitable surface environment [*Pollack et al.*, 1987; *Jakosky and Phillips*, 2001].

Previous spacecraft measurements have established that atmospheric ions escape the planet and have been used to map the spatial distribution of ions around the planet. The Phobos 2 mission provided the first direct measurements of escaping O^+ ions [*Lundin et al.*, 1990] and presented the idea that there is spatial structure to the escaping ion energies and fluxes [*Kallio et al.*, 1995]. Mars Express has measured planetary ions for an entire solar cycle and continues to provide measurements of escape rates and the spatial distribution of ions downstream from and near the planet [e.g., *Barabash et al.*, 2007; *Fränz et al.*, 2007; *Lundin et al.*, 2008; *Fränz et al.*, 2010; *Nilsson et al.*, 2010, 2011; *Ramstad et al.*, 2015]. These measurements lead to the present understanding of the existence of a variety of acceleration processes for ions and different channels for escape [e.g., *Dubinin et al.*, 2011]. Estimates of the total present-day ion escape rate range from $\sim 10^{23}\ s^{-1}$ to $3 \times 10^{25}\ s^{-1}$ [*Dubinin et al.*, 2011, and references therein]. Discrepancies in the determination of escape rate depend partly upon the energy range of particles considered. Both escape rates and the spatial distribution of ions near Mars provide important constraints for models of ion loss from Mars. These models, validated by observations, can be used to estimate atmospheric loss rates at earlier epochs in Martian history [*Lillis et al.*, 2015].

The Mars Atmosphere and Volatile EvolutioN (MAVEN) mission arrived at Mars in September 2014 and began making measurements of the Martian upper atmosphere and escaping particles, with the objective of

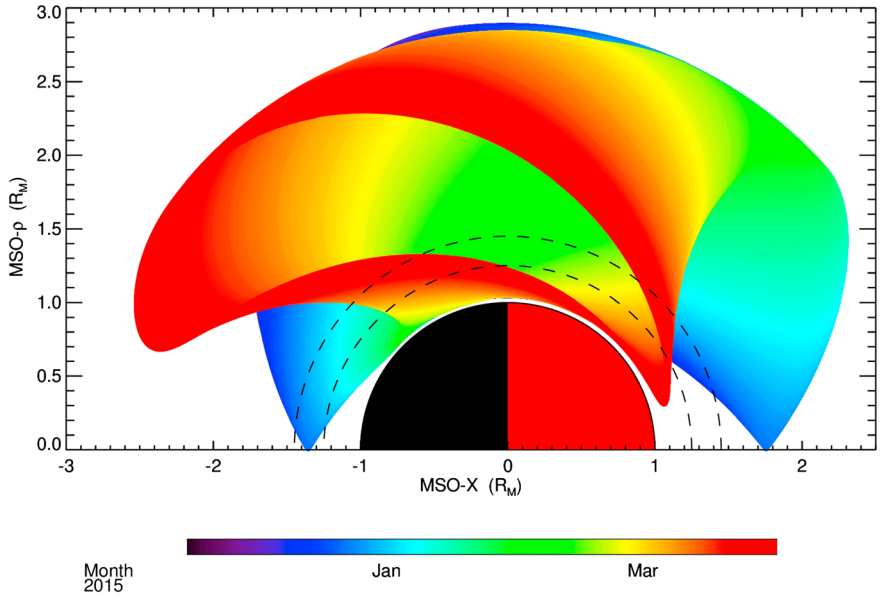

Figure 1. MAVEN's orbit coverage from 16 November 2014 to 1 April 2015. Coverage is shown in cylindrical coordinates relative to the Mars-Sun line, with each orbit chronologically overplotted. Dashed lines indicate the inner and outer boundaries of a spherical shell around Mars used to analyze ion fluxes for this study.

evaluating the importance of atmospheric escape in shaping Martian climate [*Jakosky et al.*, 2015]. MAVEN should build upon the successes of previous missions in three ways. First, MAVEN carries instruments that directly measure the solar and solar wind drivers of escape, including magnetic field measurements that can be used to organize the spatial distribution of escaping ions. Second, MAVEN's planetary ion measurements typically occur at higher cadence (16 s or better) than recent missions, allowing better determination of the 3-D distribution of ions on smaller spatial and temporal scales. Third, as a mission entirely dedicated to the upper atmosphere and escape, MAVEN carries a full complement of instruments capable of probing the physics of ion acceleration. One goal of MAVEN is to use the measured variability in atmospheric escape rates via each loss process to extrapolate back in time [*Jakosky et al.*, 2015; *Lillis et al.*, 2015].

Here we present the first results of an effort to spatially map the measured fluxes of planetary ions observed by MAVEN near Mars in a way that allows an estimation of the ion escape rate. We separately map ions moving toward and away from the planet and construct maps of the net flux of ions. We use these maps to place initial constraints on present-day global escape rates and place them in context with previous measurements.

2. Methodology

Our analysis includes measurements from the start of MAVEN science operations on 16 November 2014, through 1 April 2015. The orbital coverage of MAVEN for this time period is shown in Figure 1.

We map MAVEN planetary ion measurements to a closed surface around the planet, in contrast to most previously published studies. This approach is taken for two reasons: (1) we seek to evaluate the flux of ions both leaving and approaching the planet, suggesting the use of a closed surface, and (2) a "plume" of escaping ions detected by MAVEN apparently contains significant ion fluxes on trajectories that would not intersect the more traditional planar surface behind Mars [*Dong et al.*, 2015]. In the coming studies we plan to compare a variety of surfaces for mapping ion escape from Mars. Here we choose a spherical surface that ranges from 1.25 to 1.45 Mars radii (R_M) or ~850–1530 km altitudes. This radial distance is chosen so that all nightside solar zenith angles are sampled on the surface, as shown in Figure 1.

We select times when MAVEN was located on the spherical shell (i.e., between 1.25 and 1.45 R_M). These periods are mapped in the often used Mars-Solar-Orbital (MSO) coordinate system in Figure 2 (left), corrected for the aberration of the solar wind at Mars by using the upstream solar wind velocity measured by the Solar Wind Ion Analyzer (SWIA) [*Halekas et al.*, 2013]. The coverage spans a relatively limited range of local times

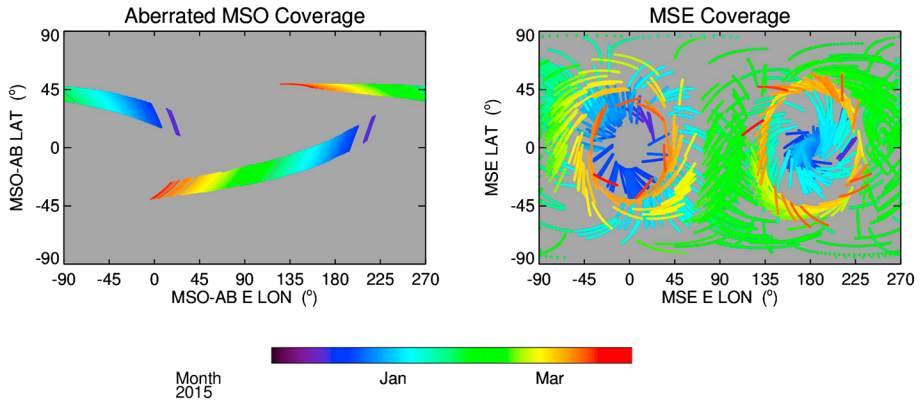

Figure 2. MAVEN orbital coverage on a shell extending from 1.25 to 1.45 R_M, for time periods from 16 November 2014 to 1 April 2015. (left) Coverage in MSO coordinates, corrected for the solar wind aberration at Mars. (right) Coverage in MSE coordinates with the upstream electric field direction parallel with the *y* axis of the plot. Dayside regions are on the left half of both panels with the subsolar point at (0,0), and nightside regions are on the right half of both panels with the antisolar point at (180,0).

and solar latitudes. Ion motion near Mars, however, is believed to be largely structured by the directions of the solar wind flow and interplanetary magnetic field (IMF). Therefore, we rotate MAVEN's location at each time into a Mars-Solar-Electric field (MSE) coordinate system, defined on an orbit-by-orbit basis using MAVEN upstream measurements of the solar wind velocity and IMF direction recorded by SWIA and the Magnetometer (MAG) [*Connerney et al.*, 2014]. MAVEN's coverage of the shell around Mars is much more complete in this coordinate system. Of necessity, we exclude time periods for which SWIA and MAG estimates of the solar wind and IMF are unavailable. This is the primary reason that we only include observations through March 2015; MAVEN's orbit precession did not allow it to observe the solar wind after this time for a period of a few months.

Measured ion fluxes are taken from the Suprathermal and Thermal Ion Composition (STATIC) instrument on MAVEN. STATIC is an electrostatic analyzer with time-of-flight measurement capability (J. McFadden et al., The MAVEN Suprathermal and thermal Ion Composition (STATIC) Instrument, submitted to *Space Science Reviews*, 2015) that can record ion fluxes as a function of energy (0.1eV–20 keV), mass (1–70 amu), azimuth direction (0–360°), and deflection angle (~±45°). We use measurements recorded when the instrument was in "pickup ion mode," which provides a good combination of energy (32 channels), mass (8 mass bins), and angular (4 defections and 16 azimuth directions) resolution. Wherever possible, archive data with 16 s cadence are used. When archive data are not available (~3.5% of the time), we use survey data with cadence of 512 s. We omit observations for which the estimated background was abnormally high or the attenuator changed state during the observation (leading to an invalid geometric factor), leaving a total of 20,836 observations over an ~4 month period.

We treat each STATIC observation in our study individually before including it in maps of ion fluxes. Our analysis treats only heavy ions, with mass/charge of 9 amu or greater. First, we apply a rough procedure to remove instrument counts from "straggling protons." Straggling, described in J. McFadden et al. (submitted manuscript, 2015), results in protons being recorded at higher masses due to the energy loss of particles in the foils used in STATIC's time-of-flight system. Sophisticated background subtraction techniques are presently being developed for STATIC data; here we take a conservative approach of subtracting 20% (a value arrived at after manual inspection of many distributions) of the counts recorded at masses less than 2.5 amu from all higher mass bins at each energy and visually inspecting the results. This likely results in a slight oversubtraction of heavy ion counts at energies where proton fluxes are greatest but is preferable to the alternative of analyzing flux in heavy ion mass bins that come from protons. Overall uncertainty in the determination of flux is estimated to be 50% or less.

We do not correct the measurements for spacecraft potential or spacecraft velocity effects. While MAVEN can measure spacecraft potential via several methods, a mature determination of spacecraft potential has not yet been incorporated into our analysis. Charging and velocity effects most strongly influence low-energy ion

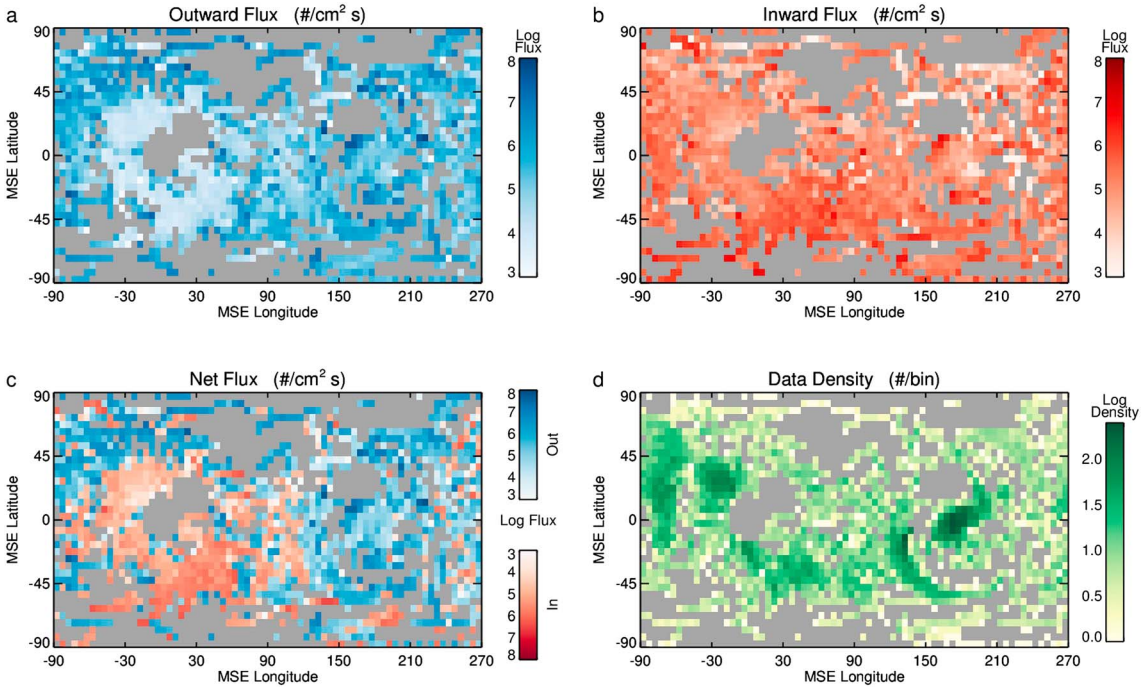

Figure 3. Measured ion fluxes mapped to a spherical shell around Mars in 5° × 5° bins, in the same MSE coordinate system used in Figure 2. The subsolar point is at (0,0) and the antisolar point at (180,0). (a) Median outward ion fluxes. (b) Median inward ion fluxes. (c) Net flux in each bin, obtained by subtracting the inward flux map from the outward flux map. (d) The number of observations in each bin.

observations. We therefore do not include measurements below 25 eV in our study. Further discussion is provided in *Harada et al.* [2015].

Finally, we separate each measured distribution into the portions moving toward or away from the planet with respect to our surface, respectively. The vector ion flux for each portion of the distribution is computed (via direct integration) and the radial component of the flux mapped into 5° × 5° spatial bins on our surface. Separate maps for incident and escaping ions are constructed.

3. Results

Figure 3 shows the results of mapping the planetary heavy ($m/q >$ ~9) ion fluxes measured by STATIC onto the spherical shell around Mars. Overall, ~68% of the surface area of the shell is covered by the maps, and a median of seven observations occupies each populated bin, with a maximum of 376 observations in a single bin. As the MAVEN mission progresses, the surface area coverage of the maps should increase, as well as the number of observations in each bin.

A map of the median outward ion flux in each bin is shown in Figure 3a. We select median values in this study as proxies for the "typical" flux in each bin and as values less likely to be influenced by extreme values than a mean flux. If we instead choose mean flux, we obtain higher values, but the relative variations in the spatial distribution of planetary ions are not significantly changed. The flux of outward ions from the central portion of the dayside of the planet is low compared to the flux on the nightside and at high northern (in MSE coordinates) dayside latitudes.

Figure 3b shows a map of the median inward flux. The inward fluxes appear to be more uniformly distributed than the outward fluxes, with the exception of the southern electric field hemisphere on the dayside where fluxes are higher than in other regions.

The net flux in each bin is obtained by taking the difference between the median outward and inward fluxes. The results are shown in Figure 3c. A few different spatial regions are evident from the figure. On the nightside of the planet, outward flux generally dominates inward flux and the net flow of particles is away from the

Table 1. Heavy Ion Rates Measured by MAVEN[a]

	Dayside	Nightside	+E Pole	−E Pole	Global
Coverage	74%	71%	57%	54%	68%
Outward rate	4.5 (2.4–9.3)	9.7 (5.8–15)	4.6 (2.5–8.3)	2.0 (1.4–3.1)	21 (12–36)
Inward rate	1.7 (.87–3.1)	1.6 (1.1–2.5)	0.42 (.29–.68)	1.1 (.84–1.6)	4.8 (3.1–7.9)
Net	2.8 (–.76–8.4)	8.1 (3.3–14)	4.2 (1.8–8.0)	0.90 (−.20–2.2)	16 (4.2–33)

[a]Total heavy ion rates through the spherical shell obtained from the maps in Figure 3, in units of 10^{23} s^{-1}.The spherical shell is divided into four regions defined in the text, and median outward, median inward, and net outward rates are computed for each, as well as global values for the entire shell. Ranges for each value are also provided, computed by summing the lower quartile and the upper quartile fluxes in each 5° × 5° spatial bin.

planet. On the dayside at low (MSE) latitudes, inward flux weakly dominates escape flux, so that the net flow of particles is toward the planet. At higher latitudes, especially in the northern (MSE) hemisphere, outward flux strongly dominates return flux.

In addition to mapping the measurements spatially, we can sum the total ion flux in various regions and use them to estimate an escape rate. Guided by Figure 3 and expectations from simulations [e.g., *Fang et al*., 2008], we choose four regions: the north and south electric field polar regions (MSE latitude $>\pm 45°$), with the remaining low latitudes divided into dayside and nightside regions. Table 1 reports the total outward, inward, and net ion rates in each region, as well as the global rates. The totals are obtained by summing the median flux in each bin, multiplied by the area of the bin. Table 1 also gives a range in rates for each region, provided as a rough estimate of the variability in each region. The range is obtained by computing the lower and upper quartile fluxes in each 5° × 5° spatial bin and then summing over all lower quartile values and upper quartile values.

Globally, the outward ion rate exceeds the inward rate by a factor of several, so that the net flow of planetary ions through the spherical shell is away from Mars. Despite some individual spatial bins being dominated by returning ion flux, the net flow is outward in all four of the large regions we have defined, though the rate from both the dayside and the southern MSE region is low and, considering the range of measured values, consistent with no net outward flow of particles. The inward rate is comparable on the dayside and nightside but is about 3 times greater in the southern MSE region than in the north. The outward rate is 2.5–3 times larger on the nightside than the dayside and ~2 times larger in the northern MSE region than the south.

Approximately 70% of the surface area of the shell has been sampled overall, but the coverage is nonuniform in each region. The results of Table 1 do not incorporate any estimate of the fluxes or escape rates in regions not yet visited by the MAVEN spacecraft. Thus, rates from the dayside and nightside are directly comparable given the similar coverage in those regions, as are rates from the north and south electric field regions. When we correct for the sampling bias by assuming that the median rate in each partially sampled region is representative of the rate in the entire region, we see that the majority of the net outward flow of ions is through the nightside (47%) and the northern electric field (31%) regions.

4. Discussion

We have been cautious to this point to refer to the mapped ion fluxes as outward and inward, but our goal is to evaluate the escape rate of planetary ions. Different spatial regions are evident in the maps in Figure 3. First, on the nightside of Mars, heavy ions escape from the planet, with a small fraction (~10–15%) returning toward the planet. Second, in the north electric field region, newly born ions escape the planet in the pickup ion plume [*Dong et al*., 2015] and are carried northward in MSE coordinates by the $-v \times B$ electric field in the plasma. This results in significant escaping fluxes seen in the dayside northern hemisphere. Third, a significant fraction of particles in the southern MSE hemisphere have trajectories that carry them inside our spherical surface. Some of these particles impact the planet in the exobase region, and others escape. We conducted test particle calculations similar to those presented in *Fang et al*. [2008], which suggested that

most of the returning particles encountering the shell on the dayside and southern MSE hemisphere impact the planet. Those that impact the planet are likely to cause sputtering of the neutral atmosphere, contributing to escape [*Lillis et al*., 2015; *Leblanc et al.*, 2015].

When constructing a global estimate of escape rates of ions with energies greater than 25 eV based on the maps presented above, we must therefore make several assumptions. The global outward rate of ions from the spherical shell is $2.1 \times 10^{24}\,s^{-1}$. Test particle calculations and global plasma models suggest that most of the particles traveling toward the planet on the nightside were ionized below the shell and thus should be represented in both the maps of escaping flux and return flux. Inward flux in the other three regions is likely to have been ionized above the shell and should not be included in estimates of escape. Thus, we subtract the return rate from only the nightside region to obtain a net escape rate of $1.9 \times 10^{24}\,s^{-1}$, which is about 20% higher than the global net rate of $1.6 \times 10^{24}\,s^{-1}$ and 10% lower than the global outward flux of ions from the planet.

We must also consider that only 70% of the spherical shell has been sampled by MAVEN so far. If we assume that the sampled bins are, on average, characteristic of the unsampled regions, then we can simply scale the measured rate to account for the unmeasured 30% of our shell. This yields a global outward escape rate of $3.1 \times 10^{24}\,s^{-1}$ and, accounting for particles returning toward Mars on the nightside, a net escape rate of $2.8 \times 10^{24}\,s^{-1}$.

These values are almost certainly an underestimate of the true planetary ion escape rate from Mars, for several reasons. First, we have omitted low-energy ions from our calculations. Analysis of Mars Express data suggests that consideration of low-energy particles increases the escape rate by factors of 2–10 (see discussion in *Dubinin et al*. [2011] and *Nilsson et al*. [2012]). Next, STATIC's field of view is not always oriented in the correct direction to measure all escaping particles [*Jakosky et al*., 2015; *Dong et al*., 2015]. We have not accounted for this in the statistical analysis above, which likely depresses the estimation of escape rate. Third, our spherical shell was set relatively close to the planet so that a wide range of solar zenith angles could be sampled on the nightside. This shell, therefore, does not capture particles ionized at high altitudes that move on trajectories that do not intersect the shell at all. MAVEN observations have detected such ions from the high-altitude corona [*Dong et al*., 2015; *Rahmati et al.*, 2015], and they are far less numerous than particles ionized at low altitudes. Finally, we have employed a conservative correction for proton straggling in the STATIC instrument, which errs on the side of removing too many heavy ion counts. Future improvements to the straggling correction should result in slightly higher planetary ion fluxes. All of these considerations lead to the assertion that the escape rates reported from this analysis should be taken as lower limits.

Escape rates have been reported several times based on Mars Express data. Using a similar energy range (>30–40 eV) to our analysis above, *Barabash et al*. [2007] obtained an escape rate 3–4 times lower than our estimate, and *Lundin et al*. [2008] derived a comparable escape rate (the highest of all previously published estimates for this energy range). They are in range with heavy ion escape rates reported for a greater range of particle energies by *Nilsson et al*. [2011] but nearly an order of magnitude lower than those reported by *Fränz et al*. [2010] for solar minimum conditions and *Ramstad et al*. [2013] for solar maximum. Both of the latter studies extended to lower energies than are considered here. It remains to be seen whether the inclusion of low-energy particles, better straggling and field-of-view correction, and different surfaces increase the MAVEN estimates of total ion escape to comparable values.

Coming efforts include corrections for the effects noted above, as well as exploration of different surfaces for evaluating escape. Already, other analyses of MAVEN data are revealing the spatial distribution of ion fluxes around Mars on different (planar) surfaces [*Dong et al*., 2015; *Harada et al.*, 2015]. Additionally, the MAVEN escape rate measurements can be compared with global models [e.g., *Ma et al*., 2014; *Dong et al*., 2014; *Modolo et al*., 2012] and can be separated by various solar and solar wind drivers, such as EUV flux, solar wind pressure (density and velocity), Mars season, and Mars orientation. MAVEN's periapsis was in the northern hemisphere for all time periods included in this study, so that coverage of the relevant regions for escape is still incomplete in geographic (e.g., with respect to crustal fields) and MSO coordinates, despite coverage being quite good in MSE coordinates. Finally, the effort here represents an analysis of the total ion escape from Mars independent of the energization process for ions. Future efforts should explore the relative importance of the various processes.

All of these influences can be explored in detail as MAVEN's orbital coverage improves. The variation of escape rates with drivers mentioned above is especially important if we wish to extrapolate the measurements to earlier epochs when the Sun and solar wind were more active and ion loss rates were likely to have been greater. We will then be able to estimate the total atmospheric ion loss over Martian history and integrate it with the loss of neutral particles to estimate the impact on Martian climate.

Acknowledgments
The MAVEN project is supported by NASA through the Mars Exploration Program, and MAVEN data are publicly available through the Planetary Data System. This research would not be possible without the diligent efforts of the spacecraft and instrument teams over many years. We further acknowledge useful conversations with E. Dubinin and M. Fraenz.

The Editor thanks two anonymous reviewers for their assistance in evaluating this paper.

References

Barabash, S., A. Fedorov, R. Lundin, and J.-A. Sauvaud (2007), Martian atmospheric erosion rates, *Science*, *315*(5811), 501–503, doi:10.1126/science.1134358.

Connerney, J. E. P., J. Espley, P. Lawton, S. Murphy, J. Odom, R. Oliversen, and D. Sheppard (2014), The MAVEN magnetic field investigation, *Space Sci. Rev.*, doi:10.1007/s11214-015-0169-4.

Dong, C., S. W. Bougher, Y. Ma, G. Tóth, A. F. Nagy, and D. Najib (2014), Solar wind interaction with Mars upper atmosphere: Results from the one-way coupling between the multifluid MHD model and the MTGCM model, *Geophys. Res. Lett.*, *41*, 2708–2715, doi:10.1002/2014GL059515.

Dong, Y., X. Fang, D. A. Brain, J. P. McFadden, J. S. Halekas, J. E. P. Connerney, S. M. Curry, Y. Harada, J. G. Luhmann, and B. M. Jakosky (2015), Strong plume fluxes observed by MAVEN: An important planetary ion escape channel, *Geophys. Res. Lett.*, doi:10.1002/2015GL065346.

Dubinin, E., M. Fraenz, A. Fedorov, R. Lundin, N. Edberg, F. Duru, and O. Vaisberg (2011), Ion energization and escape on Mars and Venus, *Space Sci. Rev.*, *162*(1), 173–211, doi:10.1007/s11214-011-9831-7.

Fang, X., M. W. Liemohn, A. F. Nagy, Y. Ma, D. L. De Zeeuw, J. U. Kozyra, and T. H. Zurbuchen (2008), Pickup oxygen ion velocity space and spatial distribution around Mars, *J. Geophys. Res.*, *113*, A02210, doi:10.1029/2007JA012736.

Fränz, M., E. Dubinin, E. Roussos, J. Woch, J. D. Winningham, R. Frahm, A. J. Coates, A. Fedorov, S. Barabash, and R. Lundin (2007), Plasma moments in the environment of Mars, *Space Sci. Rev.*, *126*(1–4), 165–207, doi:10.1007/s11214-006-9115-9.

Fränz, M., E. Dubinin, E. Nielsen, J. Woch, S. Barabash, R. Lundin, and A. Fedorov (2010), Transterminator ion flow in the Martian ionosphere, *Planet. Space Sci.*, *58*(1), 1442–1454, doi:10.1016/j.pss.2010.06.009.

Halekas, J. S., E. R. Taylor, G. Dalton, G. Johnson, D. W. Curtis, J. P. McFadden, D. L. Mitchell, R. P. Lin, and B. M. Jakosky (2013), The solar wind ion analyzer for MAVEN, *Space Sci. Rev.*, *101*, doi:10.1007/s11214-013-0029-z.

Harada, Y., et al. (2015), Marsward and tailward ions in the near-Mars magnetotail: MAVEN observations, *Geophys. Res. Lett.*, *42*, doi:10.1002/2015GL065005.

Jakosky, B. M., and R. J. Phillips (2001), Mars' volatile and climate history, *Nature*, *412*(6), 237–244.

Jakosky, B. M., et al. (2015), The Mars Atmosphere and Volatile EvolutioN (MAVEN) mission, *Space Sci. Rev.*, *21*, doi:10.1007/s11214-015-0139-x.

Kallio, E., H. Koskinen, S. Barabash, C. M. C. Nairn, and K. Schwingenschuh (1995), Oxygen outflow in the Martian magnetotail, *Geophys. Res. Lett.*, *22*(1), 2449–2452, doi:10.1029/95GL02474.

Leblanc, F., et al. (2015), Mars heavy ion precipitating flux as measured by MAVEN, *Geophys. Res. Lett.*, *42*, doi:10.1002/2015GL066170.

Lillis, R. J., et al. (2015), Characterizing atmospheric escape from Mars today and through time, with MAVEN, *Space Sci. Rev.*, doi:10.1007/s11214-015-0165-8.

Lundin, R., A. Zakharov, R. Pellinen, S. W. Barabasj, H. Borg, E. M. Dubinin, B. Hultqvist, H. Koskinen, I. Liede, and N. Pissarenko (1990), ASPERA/Phobos measurements of the ion outflow from the Martian ionosphere, *Geophys. Res. Lett.*, *17*, 873–876, doi:10.1029/GL017i006p00873.

Lundin, R., S. Barabash, M. Holmström, H. Nilsson, M. Yamauchi, M. Fraenz, and E. M. Dubinin (2008), A comet-like escape of ionospheric plasma from Mars, *Geophys. Res. Lett.*, *35*, L18203, doi:10.1029/2008GL034811.

Ma, Y. J., X. Fang, A. F. Nagy, C. T. Russell, and G. Tóth (2014), Martian ionospheric responses to dynamic pressure enhancements in the solar wind, *J. Geophys. Res. Space Physics*, *119*, 1272–1286, doi:10.1002/2013JA019402.

Modolo, R., G. M. Chanteur, and E. Dubinin (2012), Dynamic Martian magnetosphere: Transient twist induced by a rotation of the IMF, *Geophys. Res. Lett.*, *39*, L01106, doi:10.1029/2011GL049895.

Nilsson, H., E. Carlsson, D. A. Brain, M. Yamauchi, M. Holmström, S. Barabash, R. Lundin, and Y. Futaana (2010), Ion escape from Mars as a function of solar wind conditions: A statistical study, *Icarus*, *206*(1), 40–49, doi:10.1016/j.icarus.2009.03.006.

Nilsson, H., N. Edberg, G. Stenberg, and S. Barabash (2011), Heavy ion escape from Mars, influence from solar wind conditions and crustal magnetic fields, *Icarus*, doi:10.1016/j.icarus.2011.08.003.

Nilsson, H., G. Stenberg, Y. Futaana, M. Holmström, S. Barabash, R. Lundin, N. J. T. Edberg, and A. Fedorov (2012), Ion distributions in the vicinity of Mars: Signatures of heating and acceleration processes, *Earth Planets Space*, *64*(2), 135–148, doi:10.5047/eps.2011.04.011.

Pollack, J. B., J. F. Kasting, S. M. Richardson, and K. Poliakoff (1987), The case for a wet, warm climate on early Mars, *Icarus*, *71*, 203–224, doi:10.1016/0019-1035(87)90147-3.

Rahmati, A., D. E. Larson, T. E. Cravens, R. J. Lillis, P. A. Dunn, J. S. Halekas, J. E. Connerney, F. G. Eparvier, E. M. B. Thiemann, and B. M. Jakosky (2015), MAVEN insights into oxygen pickup ions at Mars, *Geophys. Res. Lett.*, *42*, doi:10.1002/2015GL065262.

Ramstad, R., Y. Futaana, S. Barabash, H. Nilsson, S. M. del Campo B, R. Lundin, and K. Schwingenschuh (2013), Phobos 2/ASPERA data revisited: Planetary ion escape rate from Mars near the 1989 solar maximum, *Geophys. Res. Lett.*, *40*, 477–481, doi:10.1002/grl.50149.

Ramstad, R., S. Barabash, Y. Futaana, H. Nilsson, X. D. Wang, and M. Holmström (2015), The Martian atmospheric ion escape rate dependence on solar wind and solar EUV conditions: I. Seven years of Mars Express observations, *J. Geophys. Res. Planets*, *120*, 1298–1309, doi:10.1002/2015JE004816.